Solar Energy Materials & Solar Cells 120 (2014) 303–309

Contents lists available at ScienceDirect

Solar Energy Materials & Solar Cells

journal homepage: www.elsevier.com/locate/solmat

Effect of replacing proton with alkoxy side chain for donor acceptor type organic photovoltaics

Kwan Wook Song [a], Min Hee Choi [a], Ho Jun Song [a], Soo Won Heo [a], Jang Yong Lee [b], Doo Kyung Moon [a,*]

[a] Department of Material Chemistry and Engineering, Konkuk University, Seoul 143-701, Republic of Korea
[b] Energy Materials Research Center, Korea Research Institute of Chemical Technology, P.O. Box 107, Yuseong, Daejeon 305-600, Republic of Korea

ARTICLE INFO

Article history:
Received 4 July 2013
Received in revised form
6 September 2013
Accepted 18 September 2013
Available online 7 October 2013

Keywords:
Alkoxy chain
Stille coupling reaction
Molecular weight
Absorption coefficient
Edge-on structure
Bulk-heterojunction polymer solar cells

ABSTRACT

Poly(quarterthiophene-alt-benzothiadiazole), PQT12oBT and PQT12BT, were synthesized through the Stille coupling reaction. The UV–visible absorption spectrum of PQT12oBT showed peaks at 535 nm; moreover, it exhibited a higher molar absorption coefficient (ε=44,000 M^{-1} cm^{-1} at 535 nm) than PQT12BT (3300 M^{-1} cm^{-1}) in chloroform solution. The optical band gap of PQT12oBT was calculated 1.74 eV in solid state. The HOMO and LUMO energy levels of PQT12oBT were −5.18 and −3.44 eV, respectively. From the results of X-ray diffraction measurements, the lamellar d-spacing of PQT12oBT in out-of-plane direction was determined to be 21.6 Å, and the π–π stacking distance between layers was found to be 4.09 Å, with a slight edge-on orientation. Bulk heterojunction-type polymer solar cells were fabricated. With a 1:1 ratio of PQT12oBT and $PC_{71}BM$, the values of open circuit voltage (V_{oc}), short circuit current density (J_{sc}), fill factor (FF), and power conversion efficiency (PCE) were found to be 0.77 V, 8.9 mA cm^{-1}, 62.4%, and 4.2%, respectively. In addition, PCE was increased up to 4.4% by the addition of 1-bromonaphthalene (1-BrNT) to the active layer.

1. Introduction

Organic electronic devices such as organic light-emitting diodes (OLEDs) [1–5], organic photovoltaic cells (OPVs) [6–10], and organic thin-film transistors (OTFTs) [11–14] have attracted significant attention owing to their easy manufacturing based on solution processes. As a result, good solubility, oxidative stability, and high charge-carrier mobility represent important properties required in active materials. OPVs have lately been gathering attention as a major research section since the introduction of the advanced molecular engineering technology of π-conjugated polymers. However, the low power conversion efficiency (PCE) of OPVs is a major obstacle. In order to increase the PCE, it is necessary to tune the optoelectronic properties of the photoactive material, i.e., the π-conjugated polymer. Methods of tuning these properties include (1) a lowering of the energy level of the highest occupied molecular orbital (HOMO) to achieve a high open-circuit voltage (V_{oc}), (2) decreasing the band gap to extend the absorption region, and (3) increasing the molecular weight [15].

One of the promising π-conjugated polymers in the field of organic solar cells was poly(3-hexylthiophene) (P3HT) because of its beneficial properties such as a high hole mobility (0.10 cm^2/V s) [16], enhanced photostability [17], and an improved optical absorption in the visible region. Recently, solution processable regioregular poly(3,3‴-didodecylquaterthiophene) (PQT-12) was reported to have a lower HOMO level ($HOMO_{PQT12}$ = −5.24 eV, $HOMO_{P3HT}$ = −5.00 eV), better oxidative stability and faster transistor mobility (0.18 cm^2/V s) [18–22] than P3HT. In spite of these merit, the PCEs of PQT-12 and its derivatives were reached up to 3.2% [22–26]. Especially, these polymers like PQT-12 and PBTTT [12] had unsubstituted conjugated moieties as bithiophene and thienothiophene in backbone resulted in much better oxidative stability and hole mobility. These moieties promoted favorable interdigitation of side chains. Because of interdigitation, well-organized intermolecular 3D ordering and large crystalline domains would be available [27].

Because of harvesting visible and near infrared wavelength photons, low band-gap conjugated materials have been interested. To make low band gap materials is the incorporation of strong electron donating and electron accepting moieties along the conjugated backbone. Typical acceptor units are 2,1,3-benzothiazole (BT). Geng et al. reported on the polymers, poly(oligothiophene-alt-benzothiadiazole) (PT*n*BT) (*n*=2–6) which include oligothioephen and BT, with a PCE of 0.93–2.23% [28]. Many studies have focused on increasing the molecular weight and solubility by using DTBT derivatives in which side chains are introduced [29–36].

In this work, we synthesized low band-gap polymer, poly [quarterthiophene-alt-benzothiadiazole] (PQT12oBT), with octyloxy chains in the benzothiadiazole (oBT). Due to the introduction of octyloxy chain, the molecular weight and the solubility of PQT12oBT

* Corresponding author. Tel.: +82 2 450 3498; fax: +82 2 444 0765.
E-mail address: dkmoon@konkuk.ac.kr (D.K. Moon).

0927-0248/$ - see front matter © 2013 Elsevier B.V. All rights reserved.
http://dx.doi.org/10.1016/j.solmat.2013.09.023

were increased rather than those of PQT12BT. A number-average molecular weight of 43 kg/mol and molar absorption coefficient ($\varepsilon = 4.4 \times 10^4\ M^{-1}\ cm^{-1}$ at 535 nm) of PQT12oBT was confirmed.

2. Results and discussion

Scheme 1 shows the chemical structure and the synthesis process of monomers and polymers. Poly(3,3‴-didodecyl-quaterthiophene-5,5‴-diyl)-alt-(5,6-octyloxy-2,1,3-benzothiadiazole-4,7-diyl) (PQT12oBT) was polymerized by the Stille coupling reaction using M1 and M8 to introduce octyloxy side chains to BT. Also, poly((3,3‴-didodecyl quaterthiophene-5,5‴-diyl)-alt-(2,1,3-benzothiadiazole-4,7-diyl)) (PQT12BT) was polymerized by the same method using M1 and M6. PQT12oBT showed a homogeneous phase during polymerization, whereas precipitation occurred after 3 h in case of PQT12BT. The solution was poured into methanol and filtered. The obtained powders were purified using a soxhlet apparatus with methanol and acetone. Finally, the polymer was recovered from the chloroform soluble fraction and precipitated in methanol. Dark-violet powders were obtained. PQT12oBT showed a high yield (97%), whereas PQT12BT manifested only a low yield (29%). PQT12oBT and PQT12BT could be well dissolved in ordinary organic solvents, such as chlorobenzene and o-dichlorobenzene. The structure of synthesized PQT12oBT has been confirmed by ^{1}H NMR (Fig. S1 in the Supporting information).

Gel permeation chromatography (GPC) analysis of the two polymers showed different molecular weight and polydispersity, as listed in Table 1. PQT12BT was precipitated but PQT12oBT was well-soluble in toluene during polymerization. Thus, the growth of PQT12BT was limited. But, the number of molecular weight of PQT12BT was 43 kg/mol and PQT12oBT showed an unusually high molecular weight distribution (PDI = 8.83) with a bimodal distributions due to aggregation. Bo et al. reported that low molecular weight of polymer was probably due to the poor solubility in the organic solvents used in polycondensation and polymer was precipitated from the solvent during the polymerization [33]. Usually, such a weight distribution does not occur in a C–C coupling polymerization reaction between molar equivalents of two divalent monomers [37]. The results of thermogravimetric analysis (TGA) and differential scanning calorimetry (DSC) (Fig. S3) revealed that PQT12oBT showed 5% thermal weight loss at 305 °C and a melting temperature of 201 °C [38] corresponding to a high thermal stability.

Fig. 1 shows the UV–visible spectra of the polymers in solution and in normalized films. Maximum absorption peaks (at a corresponding wavelength λ_{max}) of PQT12BT and PQT12oBT in $CHCl_3$ solution at a concentration of 10 μg/mL appeared at 548 nm and 535 nm, respectively. The absorption coefficients at the absorption maxima of PQT12BT and PQT12oBT were calculated to 3.3×10^3 and $4.4 \times 10^4\ M^{-1}\ cm^{-1}$, respectively. In solution, both polymers are red-shifted compared to the UV-visible spectrum of PQT12 ($\lambda_{max} \sim 530$ nm) reported by Sellinger et al. [22]. Due to the introduction of benzothiadiazole derivatives, D–A type polymers were synthesized and the absorption range of polymers was expanded. As shown in Fig. 1(b), λ_{max} of PQT12BT and PQT12oBT

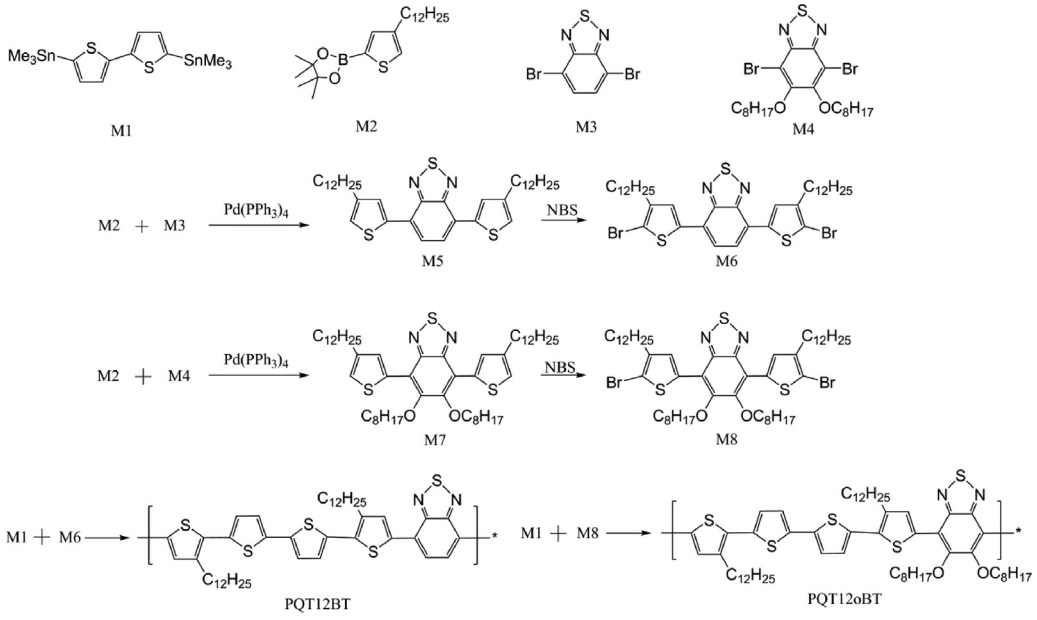

Scheme 1. Synthesis route to PQT derivatives.

Table 1
Molecular weight, optical, and electrochemical data for polymers.

	Mn[a] [kg/mol]	PDI[a]	UV–visible absorption				Cyclic voltammetry		DFT
			Solution		Film				
			λ_{max} [nm]	λ_{max} [nm]	λ_{onset} [nm]	E_g^{op}[b] [eV]	E_{onset}^{ox} (V)/HOMO [eV]	LUMO[c] [eV]	Calcd. HOMO [eV]
PQT12BT	5.0	1.52	548	577	747	1.66	0.85/−5.11	−3.45	−4.64
PQT12oBT	43.0	8.83	535	581	710	1.74	0.92/−5.18	−3.44	−4.65

[a] Determined by GPC in tetrahydrofuran (THF) using polystyrene standards.
[b] Calculated from the intersection of the tangents at the low energetic side of the absorption spectrum and the baseline.
[c] LUMO = HOMO + E_g^{op}.

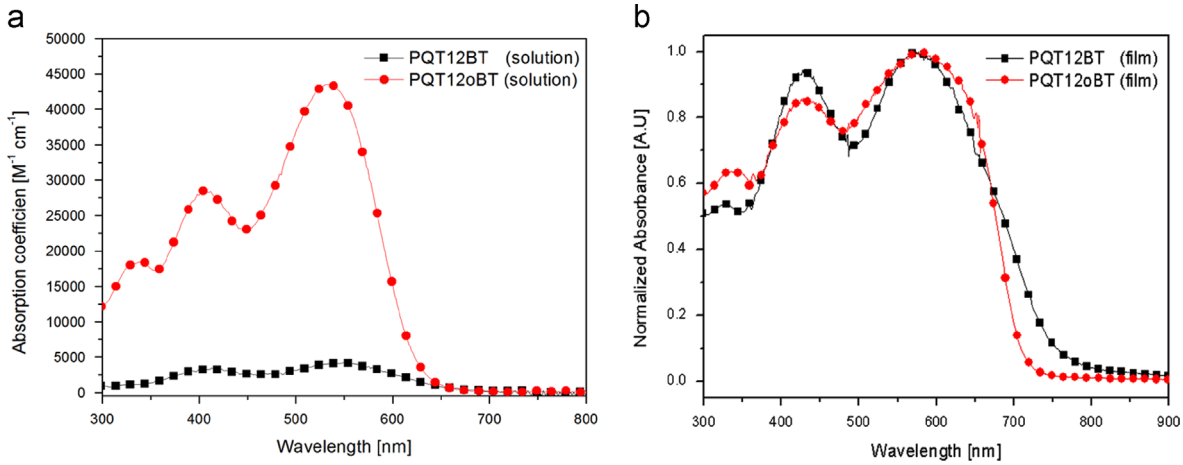

Fig. 1. UV–visible absorption spectra of polymers (a) in solution at a concentration of 10 μg/mL (left) and (b) in form of normalized films (right).

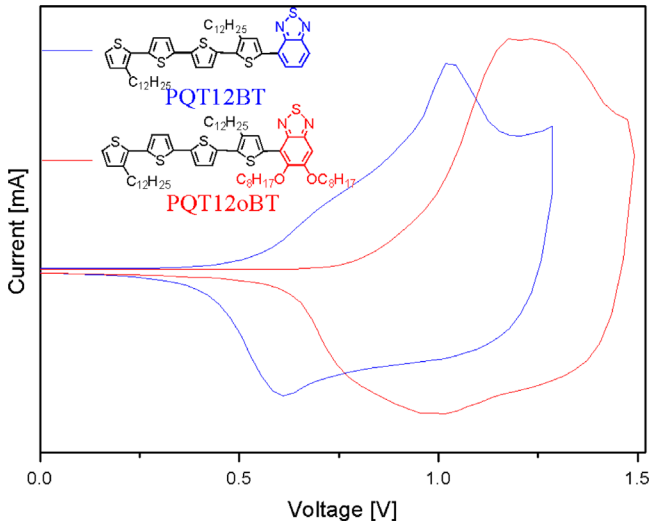

Fig. 2. Cyclic voltammograms of the polymers under consideration.

in the solid state is 577 nm and 581 nm and thus red-shifted by 29 nm and 46 nm, respectively, compared to the solution state. This red-shift is originated from the more extended delocalization of π-electrons in the D–A system [39]. The optical band gap of PQT12oBT was calculated to 1.74 eV, which is slightly higher than that of PQT12BT (1.66 eV). The optical band gaps of the two polymers were smaller than that of PQT-12 (1.90 eV) [22].

The cyclic voltammogram (CV) plots of PQTBT and PQT12oBT are shown in Fig. 2. The polymer film, drop-coated on an indium tin oxide (ITO) glass, was scanned in 0.1 M Bu_4NBF_4 solution in anhydrous acetonitrile. Based on the electrochemical oxidation onsets of PQT12BT and PQT12oBT (0.85 V and 0.92 V), the HOMO energy levels of the polymers were calculated to −5.11 eV and −5.18 eV respectively [40]. Therefore, a lowering of the HOMO energy level in polymers is possible not only for QT with side chains but also in the present case of BT with alkoxy side chains. Yi et al. explained that by introducing alkoxy side chains to BT, the HOMO level of the polymer is lowered due to a reduced electronic delocalization along the polymer backbone, and the simultaneously increased LUMO level of the polymer is explained by a weaker electron acceptability of benzothiadiazole moieties [41]. Alkoxy substitution at aromatic benzene ring has been known as strongly activating electron donating group in organic chemistry. Electron donating group activates delocalized π system by increasing the electron density at the ortho- and para- positions on the ring through a resonance donating effect. For the same reason, the HOMO level of PQT12oBT is slightly lower by 0.07 eV than that of PQT12BT. Thus, the octyloxy chain brings about an increasing oxidation potential, matching with the result of our previous study on the reduction of HOMO energy levels induced by an increase of donor groups in the main chain [42]. The HOMO levels of the polymers were similar to each other, but that of PQT12oBT was slightly lower. The LUMO energy level in PQT12oBT was calculated to −3.44 eV based on the difference between the HOMO energy level and the optical band gap.

DFT calculations were performed using the software Gaussian 09 with a B3LYP-type hybrid correlation functional and a split valence 6–31 G(d) basis set [29]. Fig. 3 shows the calculated HOMO and LUMO orbitals of oligomers containing two repeating units that were taken as a model. The dodecyl side chain of QT was computed by simplifying it to an ethyl chain. The HOMO orbitals were delocalized over the whole polymer backbones, whereas the LUMO orbitals were localized on the benzothiadiazole moiety, indicating a strong electron-withdrawing effect. In the case of PQT12oBT, HOMO level (−4.65 eV) and LUMO level (−2.52 eV) were observed by calculation. As shown in Fig. S4 of the Supporting information, the HOMO level (−6.13 eV) of oBT is higher than that (−6.64 eV) of BT. Likewise, the LUMO level (−1.95 eV) of oBT was increased in comparison to that (−2.35 eV) of BT. Thus, the HOMO and LUMO levels of oBT are increased by alkoxy side chains due to a reduced electronic delocalization along the polymer backbone and a weakening of the electron acceptability. As shown in Fig. S5, the UV–visible spectra of monomers and polymers were calculated on the basis of time-dependant DFT (TD-DFT). In Fig. S5 (a), the UV–visible spectrum of oBT had an almost six times higher intensity than that of BT. However, unlike the results of the UV–visible measurement, the calculated UV–visible spectrum of the PQT12oBT dimer revealed a low intensity compared with that of the PQT12BT dimer in Fig. S5(b). This may be attributed to the molecular weight of the polymers. As evidenced by Fig. S5(c), the intensity of UV–visible spectra is dependent on the molecular weights. Thus, the UV–visible spectral intensities of PQT12oBT with a high molecular weight are increased compared with those of PQT12BT in Fig. S5(d). As a result, like the measurements of the UV–visible spectra shown in Fig. 1(a), the absorption coefficient of PQT12oBT was increased because of the introduction of octyloxy chains. Moreover, Osaka et al. [43] showed the structure of PQT12BT to be bent, with an average dihedral angle of around 10°. By contrast, PQT12oBT has a dihedral angle of more than 30°. Despite such a high dihedral angle, PQT12oBT showed good π–π stacking characteristics (46 nm red-shift in the UV–visible spectrum of the

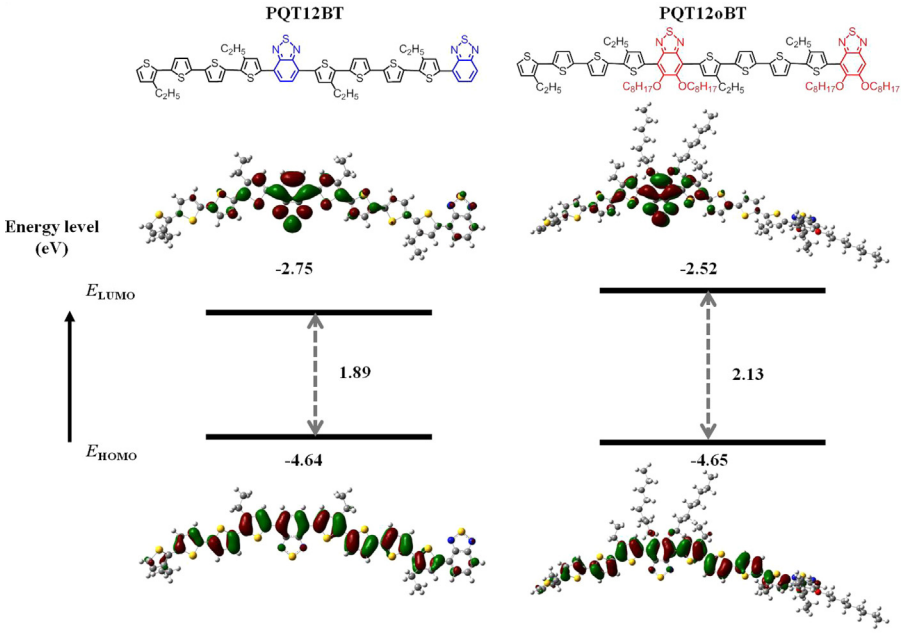

Fig. 3. Calculated LUMO and HOMO orbitals for the dimer models of the polymers.

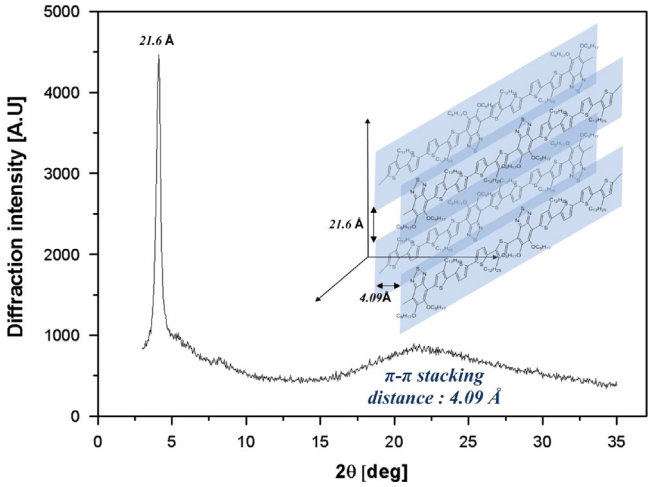

Fig. 4. X-ray diffraction pattern of drop-casted PQT12oBT film.

film). This result can be explained on the basis of interdigitated main chains, as reported by Keg, et al. [44].

Fig. 4 shows the result of the X-ray diffraction measurement to analyze the long-range ordered structure of PQT12oBT. Polymer layers were fabricated by drop casting on the glass using PQT12oBT solution dissolved in ortho-dichlorobenzene (ODCB, 10 mg/mL). In the out-of-plane direction of PQT12oBT, a sharp diffraction peak (100) was observed at 4.08°, which indicates the formation of an ordered lamellar structure by conventional edge-on stacking. The lamellar *d*-spacing (d_1) was 21.8 Å ($\lambda = 2d$ [sin θ]). In (010) direction, related to $\pi-\pi$ stacking, a broad diffraction intensity centered at approximately 21.3° was detected with a corresponding $\pi-\pi$ stacking distance (d_π) of 4.09 Å, similar to the result for $\pi-\pi$ stacking ($d_\pi = 4.0-4.4$ Å) of fluorene–thiophene. The benzene–thiophene linkage has a twisted structure compared with the thiophene–thiophene linkage [15]. PQT12oBT chains in the thin films have a slight preference for edge-on orientation. Unlike the case of PQT12, side chain ordering did not take place [45]. Therefore, the polymer backbone was twisted and got flexible due to the insertion of octyloxy chains between the ordered QT side chains.

The photovoltaic properties of PQT12oBT were measured after fabricating an ITO/PEDOT:PSS/PQT12oBT:$PC_{71}BM$/LiF/Al-structured PSC device. Fig. 5(a) and (b) shows the *J–V* curves and the incident photon conversion efficiency (IPCE) of these devices. An active layer was fabricated after spin coating for 30 s with an active area set to 4 mm^2. A blend of the polymer and $PC_{71}BM$ was dissolved in o-DCB, filtered through a 0.45 μm poly(tetrafluoroethylene) (PTFE) filter, and spin coated at 500–1100 rpm for 30 s. The active layers were pre-annealed at 120 °C for 10 min before electrode deposition. All fabricated devices were encapsulated in a glove box, and the *J–V* characteristics were measured under ambient atmosphere. The results are summarized optimized device performance in Table 2 and S1. The non-annealed device showed only 2.6% of PCE. The devices showed the best PCE (4.2%) with a J_{sc} of 9.2 mA/cm^2, V_{oc} of 0.77 V and a fill factor of 62.4% under illumination of AM1.5G, 100 mW/cm^2. In addition, PCE was increased up to 4.4% by adding 5 wt% of 1-bromonaphthalene (1-BrNT) to the active layer.

The PSC device of PQT12BT was not fabricated because of low yield. In Fig. 5(b), it has been confirmed that at wavelength of 400–500 nm, a photocurrent conversion of more than 45% was achieved by a donor polymer. In case of a device with 1-BrNT additive, however, the external quantum efficiency (EQE) and J_{sc} were slightly increased around 600 nm. In Fig. S5 and Table S1, according to the ratio of the $PC_{71}BM$ acceptor, *J–V* curves and IPCE spectra are shown, thus summarizing the device characterization.

The morphologies of polymer/$PC_{71}BM$ blend films were observed by atomic force microscopy (AFM) and are shown in Fig. 6. A large phase separation reduces charge separation and results in a low photocurrent by increasing the exciton diffusion length and, in turn, the recombination of charge [6]. Therefore, when the polymer-$PC_{71}BM$ ratio is increased to 1:2, a large phase separation appears and the photocurrent is reduced compared to the device with a 1:1 ratio of the active layer. The same result was observed for the current density and IPCE of the device, as listed in Table 2.

3. Conclusions

In this study, PQT12oBT was successfully synthesized through the Stille coupling reaction. The synthesized polymer, PQT12oBT, dissolved

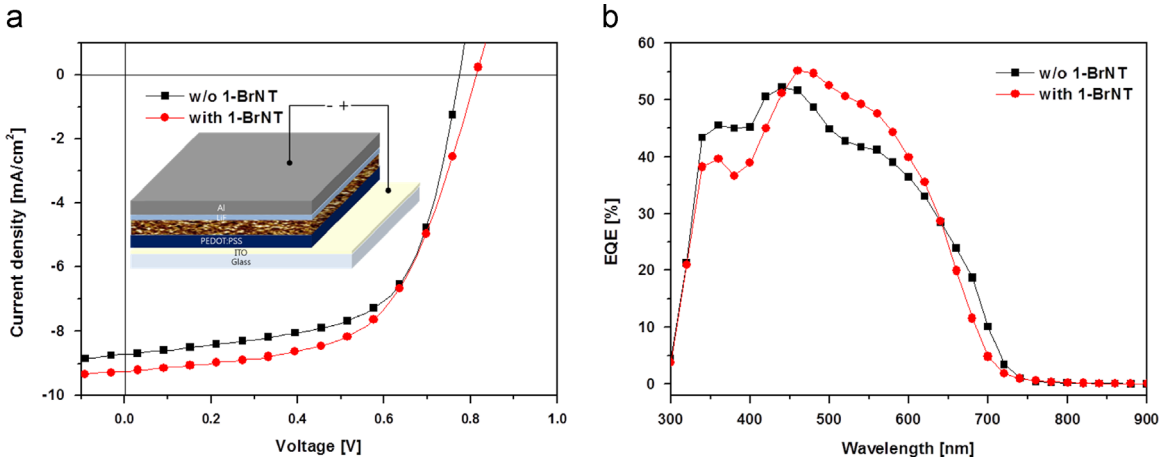

Fig. 5. (a) *J–V* curves of PSC based on PQT12oBT:$PC_{71}BM$ (1:1, w/w) under illumination of AM 1.5 G, 100 mW/cm^2. (b) The IPCE spectra of PSC based on PQT12oBT:$PC_{71}BM$ (1:1, w/w).

Table 2
Photovoltaic properties of PQT12oBT.

Additive	$PC_{71}BM$ ratios (w:w)	V_{oc} [V]	J_{sc} [mA/cm^2]	FF [%]	PCE [%]
None	1:1	0.77	8.7	62.4	4.2
5 wt% 1-BrNT	1:1	0.82	9.2	58.2	4.4

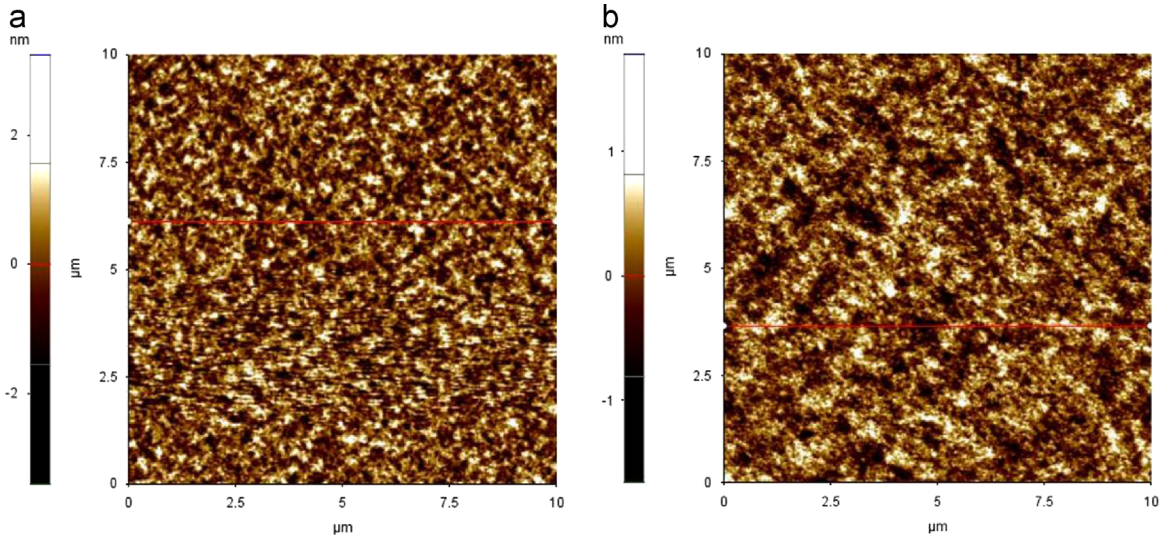

Fig. 6. AFM images (10 × 10 μm^2) of PQT12oBT/$PC_{71}BM$ films with a ratio of (a) 1:1 and (b) 1:2.

in generic organic solvents and showed a Mn of 43 kg/mol. PQT12oBT showed a low band gap (1.74 eV) and a reduction of the HOMO level to −5.18 eV. In the out-of-plane direction of PQT12oBT, the results of X-ray diffraction measurements showed a lamellar *d*-spacing of 21.6 Å and 4.09 Å of π–π stacking distance. Moreover, PQT12oBT showed a slight edge-on orientation. The device fabricated with a PQT12oBT:$PC_{71}BM$ structure (1:1, w/w) showed the best PCE in the range of 4.2–4.4%.

4. Experimental section

4.1. Materials

All starting materials were purchased from Sigma-Aldrich and Alfa Aesar and were used without further purification. Toluene and tetrahydrofuran (THF) were distilled from benzophenone ketyl and sodium. 5,5′-bis(trimethylstannyl)-2,2′-bithiophene (M1) [46], 2-(4-dodecylthiophen-2-yl)-4,4,5,5-tetramethyl-1,3,2-dioxaborolane(M2) [47], 4,7-dibromo-2,1,3-benzothiadiazole(M3) [48], 4,7-dibromo-5,6-bis(octyloxy)-2,1,3-benzothiadiazole(M4) [49], 4,7-bis(4-dodecylthiophen-2-yl)-2,1,3-benzothiadiazole(M5), 4,7-bis(5-bromo-4-dodecylthiophen-2-yl)-2,1,3-benzothiadiazole(M6), 4,7-bis(4-dodecylthiophen-2-yl)-5,6-bis(octyloxy)-2,1,3-benzothiadiazole(M7), and 4,7-bis(5-bromo-4-dodecylthiophen-2-yl)-5,6-bis(octyloxy)-2,1,3-benzothiadiazole(M8) [34,50] were prepared according to the methods reported in the literature.

4.2. Synthesis of polymers

To a mixture of M1 (0.093 g), M8 (0.2 g), tris(dibenzylideneacetone)dipalladium(0) (Pd_2dba_3) (2.3 mg, 1.3 mol%) and tri-(o-tolyl)

phosphine (3.8 mg) were dissolved in dry toluene (10 mL). The mixture was vigorously stirred at 100 °C for 48 h under a nitrogen atmosphere. After the synthesis was completed, end-capping was successively performed by 2-bromo-thiophene and 2-tributyl-stannyl-thiohpene. The mixture was cooled to room temperature, it was poured into water and separated and washed with aqueous HCl, ammonium solution and deionized water. Then, the solvent was removed under reduced pressure and the organic fraction was precipitated in methanol. The polymer was further purified by washing in methanol and acetone in a Soxhlet apparatus for 24 h. The chloroform part was reprecipitated with methanol and filtrated and, then, dried under reduced pressure at 60 °C. (0.22 g, 97%) δ_H (400 MHz; $CDCl_3$; Me4Si): 0.85–0.89 (m, 12H), 1.26–1.38 (m, 54H), 1.79 (s, 4H), 2.01 (s, 4H), 2.91 (s, 4H), 4.19 (s, 4H), 7.16–7.20 (d, 4H), 8.46 (s, 2H). GPC: Mn=43 kg/mol, Mw=381 kg/mol, PDI=8.83, Found: C, 70.20; H, 8.79; N, 2.64; S, 15.27; O, 3.13. Calcd. for $C_{62}H_{90}N_2O_2S_5$: C, 70.40; H, 8.77; N, 2.65; S, 15.16; O, 3.03%.

PQT12BT was synthesized according to the same procedure as PQT12oBT with the respective monomers (M1 and M6). Yield: 0.040 g, 29%. GPC: Mn=5 kg/mol, Mw=7.7 kg/mol, PDI=1.52

4.3. Measurements

The ^{1}H NMR (400 MHz) spectra were recorded using a Bruker AMX400 spectrometer using a solution of the polymer and $CDCl_3$ and the chemical shifts were recorded in units of ppm with TMS as internal standard. The absorption spectra were recorded using an Agilent 8453 UV–visible spectroscopy system. The chloroform solutions were used for the UV–visible spectroscopy measurements at a concentration of 10 mg/ml. The films were drop-coated from the chloroform solution onto a quartz substrate. All GPC analyses were carried out using THF as eluent and a polystyrene standard as reference. The TGA measurements were performed using a TA Instrument 2050. The cyclic voltammetric results were produced using a Zahner IM6eX electrochemical workstation with a 0.1 M acetonitrile (substituted with nitrogen for 20 min) solution containing tetrabutylammonium hexafluorophosphate (Bu_4NPF_6) as electrolyte at a constant scan rate of 50 mV/s. ITO, a Pt wire, and silver/silver chloride (Ag in 0.1 M KCl) were used as the working, counter, and reference electrodes, respectively. The electrochemical potential was calibrated against ferrocene Fc/Fc^+. The HOMO levels of the polymers were determined using the oxidation onset value. Onset potentials are values obtained from the intersection of the two tangents drawn at the rising and the baseline current of the CV curves. The LUMO levels were calculated from the differences between the HOMO energy levels and the optical band gaps, which were determined using the UV–visible absorption onset values of the films. The current density–voltage (J–V) curves of the photovoltaic devices were measured using a computer controlled Keithley 2400 source measurement unit (SMU) that was equipped with a Peccell solar simulator under illumination of AM 1.5 G (100 mW/cm^2). Topographic images of the active layers were obtained through atomic force microscopy (AFM) in tapping mode under ambient conditions using an XE-100 instrument.

Supporting Information

^{1}H NMR spectra of monomers and PQT12oBT, GPC diagram, Gaussian calculations of acceptor units, calculated UV–visible spectra of monomers and polymers using the TD-DFT method, and photovoltaic performance of bulk heterojunction (BHJ) solar cells.

Competing interest

The authors declare no competing financial interest.

Acknowledgments

This research was supported by a Grant from the Fundamental R&D Program for Core Technology of Materials funded by the Ministry of Knowledge Economy, Republic of Korea. This work was also supported by the National Research Foundation of Korea Grant funded by the Korean Government (MEST) (NRF-2009-C1AAA001-2009-0093526).

Appendix A. Supporting information

Supplementary data associated with this article can be found in the online version at http://dx.doi.org/10.1016/j.solmat.2013.09.023.

References

[1] R.H. Friend, R.W. Gymer, A.B. Holmes, J.H. Burroughes, R.N. Marks, C. Taliani, D.D.C. Bradley, D.A.D. Santos, J.L. Bredas, M. Logdlund, W.R. Salaneck, Electroluminescence in conjugated polymers, Nature 397 (1999) 121–128.
[2] G. Gustafsson, Y. Cao, G.M. Treacy, F. Klavetter, N. Colaneri, A.J. Heeger, Flexible light-emitting diodes made from soluble conducting polymers, Nature 357 (1992) 477–479.
[3] M.M. Alam, S.A. Jenekhe, Polybenzobisazoles are efficient electron transport materials for improving the performance and stability of polymer light-emitting diodes, Chemistry of Materials 14 (2002) 4775–4780.
[4] W. Lu, J. Kuwabara, T. Kanbara, Polycondensation of dibromofluorene analogues with tetrafluorobenzene via direct arylation, Macromolecules 44 (2011) 1252–1255.
[5] H.J. Song, J.Y. Lee, I.S. Song, D.K. Moon, J.R. Haw, Synthesis and electroluminescence properties of fluorene–anthracene based copolymers for blue and white emitting diodes, Journal of Industrial and Engineering Chemistry 17 (2011) 352–357.
[6] J.-Y. Lee, W.-S. Shin, J.-R. Haw, D.-K. Moon, Low band-gap polymers based on quinoxaline derivatives and fused thiophene as donor materials for high efficiency bulk-heterojunction photovoltaic cells, Journal of Materials Chemistry 19 (2009) 4938–4945.
[7] J.-Y. Lee, S.-H. Kim, I.-S. Song, D.-K. Moon, Efficient donor–acceptor type polymer semiconductors with well-balanced energy levels and enhanced open circuit voltage properties for use in organic photovoltaics, Journal of Materials Chemistry 21 (2011) 16480–16487.
[8] F.C. Krebs, Polymer solar cell modules prepared using roll-to-roll methods: knife-over-edge coating, slot-die coating and screen printing, Solar Energy Materials and Solar Cells 93 (2009) 465–475.
[9] C.S. Tao, J. Jiang, M. Tao, Natural resource limitations to terawatt-scale solar cells, Solar Energy Materials and Solar Cells 95 (2011) 3176–3180.
[10] J. Kuwabara, Y. Nohara, S.J. Choi, Y. Fujinami, W. Lu, K. Yoshimura, J. Oguma, K. Suenobu, T. Kanbara, Direct arylation polycondensation for the synthesis of bithiophene-based alternating copolymers, Polymer Chemistry 4 (2013) 947–953.
[11] B.-L. Lee, T. Yamamoto, Syntheses of new alternating CT-type copolymers of thiophene and pyrido[3,4-b]pyrazine units: their optical and electrochemical properties in comparison with similar CT copolymers of thiophene with pyridine and quinoxaline, Macromolecules 32 (1999) 1375–1382.
[12] I. McCulloch, M. Heeney, C. Bailey, K. Genevicius, I. MacDonald, M. Shkunov, D. Sparrowe, S. Tierney, R. Wagner, W. Zhang, M.L. Chabinyc, R.J. Kline, M. D. McGehee, M.F. Toney, Liquid-crystalline semiconducting polymers with high charge-carrier mobility, Nature Materials 5 (2006) 328–333.
[13] T. Yamamoto, H. Kokubo, M. Kobashi, Y. Sakai, Alignment and field-effect transistor behavior of an alternative π-conjugated copolymer of thiophene and 4-alkylthiazole, Chemistry of Materials 16 (2004) 4616–4618.
[14] T. Yasuda, Y. Sakai, S. Aramaki, T. Yamamoto, New coplanar (ABA)n-type donor−acceptor π-conjugated copolymers constituted of alkylthiophene (Unit A) and pyridazine (Unit B): synthesis using hexamethylditin, self-organized solid structure, and optical and electrochemical properties of the copolymers, Chemistry of Materials 17 (2005) 6060–6068.
[15] H.-J. Song, D.-H. Kim, E.-J. Lee, S.-W. Heo, J.-Y. Lee, D.-K. Moon, Conjugated polymer consisting of quinacridone and benzothiadiazole as donor materials for organic photovoltaics: coplanar property of polymer backbone, Macromolecules 45 (2012) 7815–7822.
[16] H. Sirringhaus, N. Tessler, R.H. Friend, Integrated optoelectronic devices based on conjugated polymers, Science 280 (1998) 1741–1744.

[17] L.M. Popescu, P.V.T. Hof, A.B. Sieval, H.T. Jonkman, J.C. Hummelen, Thienyl analog of 1-(3-methoxycarbonyl)propyl-1-phenyl-[6,6]-methanofullerene for bulk heterojunction photovoltaic devices in combination with polythiophenes, Applied Physics Letters 89 (2006) 213507.
[18] B.S. Ong, Y. Wu, Y. Li, P. Liu, H. Pan, Thiophene polymer semiconductors for organic thin-film transistors, Chemistry: A European Journal 14 (2008) 4766–4778.
[19] Y. Wu, P. Liu, B.S. Ong, T. Srikumar, N. Zhao, G. Botton, S. Zhu, Controlled orientation of liquid-crystalline polythiophene semiconductors for high-performance organic thin-film transistors, Applied Physics Letters 86 (2005) 142102.
[20] H. Chen, Y. Lu, T.-T. Ong, X. Hu, S.-C. Ng, Synthesis, characterization, and properties of regioregular conjugated polymers containing quaterthiophene and an acceptor repeating units, Journal of Polymer Science Part A: Polymer Chemistry 47 (2009) 2163–2171.
[21] B.S. Ong, Y. Wu, P. Liu, S. Gardner, High-performance semiconducting polythiophenes for organic thin-film transistors, Journal of the American Chemical Society 126 (2004) 3378–3379.
[22] P. Vemulamada, G. Hao, T. Kietzke, A. Sellinger, Efficient bulk heterojunction solar cells from regio-regular- poly(3,3‴-didodecyl quaterthiophene)/PC70BM blends, Organic Electronics 9 (2008) 661–666.
[23] A.P. Yuen, J.S. Preston, A.-M. Hor, R. Klenkler, E.Q.B. Macabebe, E.E.v. Dyk, R.O. Loutfy, Blend composition study of poly(3,3′-didodecylquaterthiophene)/[6,6]-phenyl C_{61} butyric acid methyl ester solution processed organic solar cells, Journal of Applied Physics 105 (2009) 016105.
[24] A.J. Moulé, S. Allard, N.M. Kronenberg, A. Tsami, U. Scherf, K. Meerholz, Effect of polymer nanoparticle formation on the efficiency of polythiophene based "bulk-heterojunction" solar cells, Journal of Physical Chemistry C 112 (2008) 12583–12589.
[25] D.S. Chung, H. Kong, W.M. Yun, H. Cha, H.-K. Shim, Y.-H. Kim, C.E. Park, Effects of selenophene substitution on the mobility and photovoltaic efficiency of polyquaterthiophene-based organic solar cells, Organic Electronics 11 (2010) 899–904.
[26] H. Cha, J.W. Park, D.S. Chung, T.K. An, Y.-H. Kim, S.-K. Kwon, C.E. Park, A side chain-modified quaterthiophene derivative for enhancing the performance of organic solar cell devices, Journal of Materials Chemistry 22 (2012) 15141–15145.
[27] A. Facchetti, π-Conjugated polymers for organic electronics and photovoltaic cell applications, Chemistry of Materials 23 (2011) 733–758.
[28] W. Yue, Y. Zhao, H. Tian, D. Song, Z. Xie, D. Yan, Y. Geng, F. Wang, Poly (oligothiophene-alt-benzothiadiazole)s: tuning the structures of oligothiophene units toward high-mobility "black" conjugated polymers, Macromolecules 42 (2009) 6510–6518.
[29] H. Zhou, L. Yang, S. Xiao, S. Liu, W. You, Donor−acceptor polymers incorporating alkylated dithienylbenzothiadiazole for bulk heterojunction solar cells: pronounced effect of positioning alkyl chains, Macromolecules 43 (2010) 811–820.
[30] H. Zhou, L. Yang, S.C. Price, K.J. Knight, W. You, Enhanced photovoltaic performance of low-bandgap polymers with deep LUMO levels, Angewandte Chemie International Edition 49 (2010) 7992–7995.
[31] X. Wang, Y. Sun, S. Chen, X. Guo, M. Zhang, X. Li, Y. Li, H. Wang, Effects of π-conjugated bridges on photovoltaic properties of donor-π-acceptor conjugated copolymers, Macromolecules 45 (2012) 1208–1216.
[32] P.M. Oberhumer, Y.-S. Huang, S. Massip, D.T. James, G. Tu, S. Albert-Seifried, D. Beljonne, J. Cornil, J.-S. Kim, W.T.S. Huck, N.C. Greenham, J.M. Hodgkiss, R. H. Friend, Tuning the electronic coupling in a low-bandgap donor–acceptor copolymer via the placement of side-chains, The Journal of Chemical Physics 134 (2011) 114901.
[33] W. Li, R. Qin, Y. Zhou, M. Andersson, F. Li, C. Zhang, B. Li, Z. Liu, Z. Bo, F. Zhang, Tailoring side chains of low band gap polymers for high efficiency polymer solar cells, Polymer 51 (2010) 3031–3038.
[34] C. Du, C. Li, W. Li, X. Chen, Z. Bo, C. Veit, Z. Ma, U. Wuerfel, H. Zhu, W. Hu, F. Zhang, 9-Alkylidene-9H-fluorene-containing polymer for high-efficiency polymer solar cells, Macromolecules 44 (2011) 7617–7624.
[35] G. Tu, S. Massip, P.M. Oberhumer, X. He, R.H. Friend, N.C. Greenham, W.T.S. Huck, Synthesis and characterization of low bandgap conjugated donor-acceptor polymers for polymer:PCBM solar cells, Journal of Materials Chemistry 20 (2010) 9231–9238.
[36] S. Song, Y. Jin, S.H. Kim, J. Moon, K. Kim, J.Y. Kim, S.H. Park, K. Lee, H. Suh, Stabilized polymers with novel indenoindene backbone against photodegradation for leds and solar cells, Macromolecules 41 (2008) 7296–7305.
[37] J.R. Matthews, W. Niu, A. Tandia, A.L. Wallace, J. Hu, W.-Y. Lee, G. Giri, S.C.B. Mannsfeld, Y. Xie, S. Cai, H.H. Fong, Z. Bao, M. He, Scalable synthesis of fused thiophene-diketopyrrolopyrrole semiconducting polymers processed from nonchlorinated solvents into high performance thin film transistors, Chemistry of Materials 25 (2013) 782–789.
[38] H.J. Song, J.Y. Lee, H.J. Lee, D.K. Moon, Synthesis of novel triphenylene-based discotic liquid crystals with naphthalene moiety in the side chains for photopolymerisation, Journal of Industrial and Engineering Chemistry 17 (2011) 445–449.
[39] P. Sonar, E.L. Williams, S.P. Singh, A. Dodabalapur, Thiophene–benzothiadiazole–thiophene (D–A–D) based polymers: effect of donor/acceptor moieties adjacent to D–A–D segment on photophysical and photovoltaic properties, Journal of Materials Chemistry 21 (2011) 10532–10541.
[40] K.W. Song, J.Y. Lee, S.W. Heo, D.K. Moon, Synthesis and characterization of a fluorene–quinoxaline copolymer for light-emitting applications, Journal of Nanoscience and Nanotechnology 10 (2010) 99–105.
[41] H. Yi, S. Al-Faifi, A. Iraqi, D.C. Watters, J. Kingsley, D.G. Lidzey, Carbazole and thienyl benzo[1,2,5]thiadiazole based polymers with improved open circuit voltages and processability for application in solar cells, Journal of Materials Chemistry 21 (2011) 13649–13656.
[42] J.-Y. Lee, M.-H. Choi, H.-J. Song, D.-K. Moon, Random copolymers based on 3-hexylthiophene and benzothiadiazole with induced π-conjugation length and enhanced open-circuit voltage property for organic photovoltaics, Journal of Polymer Science Part A: Polymer Chemistry 48 (2010) 4875–4883.
[43] I. Osaka, M. Shimawaki, H. Mori, I. Doi, E. Miyazaki, T. Koganezawa, K. Takimiya, Synthesis, characterization, and transistor and solar cell applications of a naphthobisthiadiazole-based semiconducting polymer, Journal of the American Chemical Society 134 (2012) 3498–3507.
[44] P. Keg, A. Lohani, D. Fichou, Y.M. Lam, Y. Wu, B.S. Ong, S.G. Mhaisalkar, Direct observation of alkyl chain interdigitation in conjugated polyquarterthiophene self-organized on graphite surfaces, Macromolecular Rapid Communications 29 (2008) 1197–1202.
[45] B.S. Ong, Y. Wu, P. Liu, S. Gardner, Structurally ordered polythiophene nanoparticles for high-performance organic thin-film transistors, Advanced Materials 17 (2005) 1141–1144.
[46] F. Brouwer, J. Alma, H. Valkenier, T.P. Voortman, J. Hillebrand, R.C. Chiechi, J.C. Hummelen, Using bis(pinacolato)diboron to improve the quality of regioregular conjugated co-polymers, Journal of Materials Chemistry 21 (2011) 1582–1592.
[47] H. Kong, D.S. Chung, I.-N. Kang, J.-H. Park, M.-J. Park, I.H. Jung, C.E. Park, H.-K. Shim, New selenophene-based semiconducting copolymers for high performance organic thin-film transistors, Journal of Materials Chemistry 19 (2009) 3490–3499.
[48] R. Yang, R. Tian, J. Yan, Y. Zhang, J. Yang, Q. Hou, W. Yang, C. Zhang, Y. Cao, Deep-red electroluminescent polymers: synthesis and characterization of new low-band-gap conjugated copolymers for light-emitting diodes and photovoltaic devices, Macromolecules 38 (2005) 244–253.
[49] D.-H. Yun, H.-S. Yoo, S.-W. Heo, H.-J. Song, D.-K. Moon, J.-W. Woo, Y.-S. Park, Synthesis and photovoltaic characterization of D/A structure compound based on N-substituted phenothiazine and benzothiadiazole, Journal of Industrial and Engineering Chemistry 19 (2013) 421–426.
[50] A. Najari, S. Beaupré, P. Berrouard, Y. Zou, J.-R. Pouliot, C. Lepage-Pérusse, M. Leclerc, Synthesis and characterization of new thieno[3,4-c]pyrrole-4,6-dione derivatives for photovoltaic applications, Advanced Functional Materials 21 (2011) 718–728.